ICLASS 2009, 11th Triennial International Annual Conference on Liquid Atomization and Spray Systems, Vail, Colorado USA, July 2009

A Numerical Method for Detailed Simulations of Atomization in Non-Isothermal Environments

P. Brady[1]*, M. Herrmann[1], and J. M. Lopez[2]
[1]Department of Mechanical and Aerospace Engineering,
and [2]Department of Mathematics and Statistics,
Arizona State University, Tempe, Arizona 85287, USA

Abstract

The atomization process of turbulent liquid jets is not well understood. Detailed numerical simulations can help study the fundamental mechanisms in regions where experimental access and analysis is virtually impossible. However, simulating atomization accurately is a huge numerical challenge since time and length scales vary over several orders of magnitude, the phase interface is a material discontinuity, and surface tension forces are singular. The Refined Level Set Grid (RLSG) method presented here is one numerical approach to simulate the primary breakup process of liquid jets and sheets in detail. With it, the liquid/gas phase interface is tracked by a level set method using an auxiliary high resolution equidistant Cartesian grid. This not only allows for application of higher-order WENO schemes retaining their full order of accuracy both for advecting and reinitializing the level set scalar, but it also provides the necessary high resolution of the phase interface geometry during topology change events in an efficient manner. When atomization occurs in non-isothermal environments, such as in combustion devices, thermal fluctuations can be significant on length scales associated with the liquid atomization process. Since the surface tension force is a function of local temperature, these thermal fluctuations may result in large local variations of the surface tension force, thereby potentially impacting the atomization process. Here, we present a numerical technique to incorporate these thermal Marangoni forces into the balanced force algorithm, together with verification and validation test cases geared towards testing the applicability of the proposed methods to the case of atomization.

Introduction

Thermal fluctuations can have a significant impact on the dynamics of liquid/gas interfaces because, for most gas/liquid combinations, both surface tension and phase transition depend strongly on the local temperature. An important technical application where both surface tension forces and phase transition are dominant is the atomization of liquid fuels for combustion processes. For combustion to occur, the liquid fuel needs to be atomized, evaporated, and mixed with an oxidizer. The ensuing chemical reactions can generate temperature variations on the order of 10^3K over small length scales of the order of 10^{-3}m. Due to the strong dependence of surface tension on temperature, the temperature fluctuations result in Marangoni forces that impact the flowfield at the gas/liquid interface, which in turn alter the interfacial temperature distribution via the induced interfacial flow [1]. Although the ratio of global inertial to surface tension forces is typically large in these applications, atomization, which is the first in the sequence of processes leading to combustion, always occurs on small scales (involving droplets which are many orders of magnitude smaller than the diameter of the initial liquid jet). At these scales, surface tension forces are dominant. Variations in temperature, resulting in variations in surface tension forces, can thus influence atomization significantly.

However, to the knowledge of the authors, there exists no detailed experimental data set analyzing the phase interface dynamics during atomization in this situation. Numerical simulations, on the other hand, can study the impact of thermally induced variations in surface tension forces and can thus help determine whether they play a role in the atomization outcome. To this end, this paper presents a numerical method for thermal Marangoni forces based on the Refined Level Set Grid (RLSG) method [2]. However, due to the lack of validation data in actual atomization situations, we study in this paper another example where the temperature-dependent surface tension influences the dynamics of phase interfaces: the thermocapillary

*Corresponding Author: peter.brady@asu.edu

motion of drops and bubbles. The study of the thermocapillary motion was first reported by [3], who determined the terminal velocity of a spherical drop in the creeping flow limit. A number of experiments have been conducted in drop towers, sounding rockets and aboard space shuttles; see the extensive review of [4]. Some of the more recent experiments have noted complicated transients and time-dependent behavior due to the effects of finite viscosity and thermal diffusivity [5–7]. In the microgravity experiments the viscous and thermal timescales of the two fluids differ by up to two orders of magnitude within a single experimental run, and so complicated temporal behavior is not surprising. All of the presently available theoretical or numerical results assume constant fluid properties, except for the surface tension which is assumed to vary linearly with temperature. The review article [4] concluded that the most important theoretical problem that needs to be addressed for an isolated drop is the consideration of the fully transient problem incorporating the dependence of physical properties on temperature.

In this paper, a numerical method for finite-volume flow solvers to consistently incorporate the Marangoni forces is verified and validated using both theoretical and experimental data.

Governing equations and numerical technique

Consider a spherical drop of one fluid with radius r_0 placed in an initially quiescent bulk fluid with an imposed (typically positive) linear temperature gradient G_T in the vertical direction. The two fluids are immiscible with, in general, different densities, viscosities and thermal properties. We shall use the initial radius of the drop, r_0, as the length scale and $G_T r_0$ as the temperature scale. For the thermocapillary motion of drops and bubbles, it is customary to use $U = \sigma_T G_T r_0/\mu_b$ as the velocity scale, where μ_b is the dynamic viscosity of the bulk phase and σ_T is the surface tension derivative with respect to temperature. This then gives $\mu_b/\sigma_T G_T$ as the time scale. The surface tension is scaled by σ_0, which for the problems considered here is the surface tension at the initial temperature at the center of the drop. Throughout, subscript d refers to properties of the drop phase and subscript b to those of the bulk phase. We shall assume that the surface tension σ between the two fluids varies linearly with slope σ_T (which for most fluids of interest is negative). With these scalings, the non-dimensional linear equation of state becomes

$$\sigma(T) = 1 + Ca(T - T_0)\,, \tag{1}$$

where T_0 is the non-dimensional initial temperature at the center of the drop, and the capillary number, which gives the relative importance of the tangential to normal stresses at the drop interface, is

$$Ca = \frac{\mu_b U}{\sigma_0} = \frac{\sigma_T G_T r_0}{\sigma_0}\,. \tag{2}$$

The non-dimensional Navier–Stokes equations governing the motion of an unsteady, incompressible, immiscible, two-fluid system, are

$$\rho_r\left(\frac{\partial \boldsymbol{u}}{\partial t} + \boldsymbol{u}\cdot\nabla\boldsymbol{u}\right) = -\nabla P + \frac{1}{Re}\nabla\cdot\mu_r\left(\nabla\boldsymbol{u} + \nabla^T\boldsymbol{u}\right) + \frac{1}{We}\boldsymbol{F}\,, \quad \nabla\cdot\boldsymbol{u} = 0 \tag{3}$$

where $\boldsymbol{u}$ is the non-dimensional velocity, P the non-dimensional pressure, the relative dynamic viscosity is $\mu_r = 1$ in the bulk phase and $\mu_r = \mu_d/\mu_b$ in the drop phase, and the relative density is $\rho_r = 1$ in the bulk phase and $\rho_r = \rho_d/\rho_b$ in the drop phase. The Reynolds and Weber numbers are

$$Re = \frac{U r_0}{\nu_b} = \frac{\sigma_T G_T r_0^2}{\mu_b \nu_b}\,, \qquad We = Re\,Ca = \frac{\rho_b r_0 U^2}{\sigma_0}\,. \tag{4}$$

The surface force $\boldsymbol{F}$, which is non-zero only at the location of the drop interface $\boldsymbol{x}_f$, is [8]

$$\frac{1}{We}\boldsymbol{F}(\boldsymbol{x}) = \frac{1}{Re}\left(\frac{1}{Ca}\kappa\delta\boldsymbol{n} + (T - T_0)\kappa\delta\boldsymbol{n} + \nabla_{||}T\delta\right)\,, \tag{5}$$

where κ and $\boldsymbol{n}$ are the local interface curvature and normal vector, $\nabla_{||}$ is the tangential surface derivative, and δ is the interface delta function. The first two terms on the right-hand side correspond to the isothermal normal stress balance and the temperature-dependent normal stress balance, and the third term corresponds to the Marangoni force. The non-dimensional heat equation for the temperature is

$$\rho_r c_{p_r}\left(\frac{\partial T}{\partial t} + \nabla\cdot(T\boldsymbol{u})\right) = \frac{1}{Ma}\nabla\cdot(k_r\nabla T)\,, \tag{6}$$

where the relative thermal conductivity $k_r = 1$ in the bulk phase and $k_r = k_d/k_b$ in the drop, the relative specific heat $c_{p_r} = 1$ in the bulk phase and $c_{p_r} = c_{p_d}/c_{p_b}$ in the drop, and the Marangoni and Prandtl numbers are

$$Ma = \frac{Ur_0\rho_b c_{p_b}}{k_b} = \frac{Ur_0}{\alpha_b} = \frac{\sigma_T G_T r_0^2}{\mu_b \alpha_b} = RePr\,, \qquad Pr = \nu_b/\alpha_b\,. \tag{7}$$

Note that the Marangoni number is equivalent to the Péclet number, Pe, for the characteristic velocity that is used in thermocapillary migration of drops or bubbles.

The simple problem of a single drop in a temperature gradient field is governed by several parameters. There are three parameters describing the dynamics: Re, Ca, and Ma (the other three, We, Pe, and Pr are dependent on these), three ratios of the material properties in the two phases: ρ_r, α_r, and μ_r, as well as a geometric parameter for the ratio of the length scale of the environment to the initial radius of the drop.

Numerics

To determine the location $\boldsymbol{x}_f$ of the phase interface we employ a level set approach by defining the level set scalar at the interface

$$G(\boldsymbol{x}_f, t) = 0\,, \tag{8}$$

with $G(\boldsymbol{x}, t) > 0$ in the drop and $G(\boldsymbol{x}, t) < 0$ in the bulk phase. Differentiating Eq. (8) with respect to time yields the level set equation,

$$\frac{\partial G}{\partial t} + \boldsymbol{u} \cdot \nabla G = 0\,. \tag{9}$$

All level set related equations are solved using the Refined Level Set Grid (RLSG) method in a separate level set solver LIT [2] using an auxiliary high-resolution G-grid with the fifth-order WENO scheme of [9] in conjunction with the third-order TVD Runge-Kutta time discretization of [10]. The phase interface curvature κ is evaluated on the G-grid using a second-order interface projection method [2].

The Navier-Stokes equations together with the temperature and continuity equation are solved by the finite volume, structured flow solver NGA [11]. The surface force in the staggered grid layout used here, needs to be evaluated at the cell faces. Its normal component is calculated following the Continuum Surface Force (CSF) model [12] that approximates $\delta\boldsymbol{n}$ by $\delta\boldsymbol{n} = \nabla\psi_{cv}$. The tangential derivative of the temperature is calculated by

$$\nabla_{||} T = \nabla T - (\nabla T \cdot \boldsymbol{n})\boldsymbol{n}\,, \tag{10}$$

where the phase interface normal vector $\boldsymbol{n}$ is evaluated on the flow solver grid by

$$\boldsymbol{n} = \frac{\nabla\psi_{cv}}{|\nabla\psi_{cv}|}\,, \tag{11}$$

where ψ_{cv} is the drop phase volume fraction of a flow solver control volume V_{cv},

$$\psi_{cv} = 1/V_{cv} \int_{V_{cv}} H(G) dV\,, \tag{12}$$

evaluated on the high resolution G grid with an algebraic expression due to [13]. This results in the surface force calculated as

$$\frac{1}{We}\boldsymbol{F}(\boldsymbol{x}) = \frac{1}{Re}\left(\frac{1}{Ca}\kappa\nabla\psi + (T - T_0)\kappa\nabla\psi + \nabla T|\nabla\psi| - \frac{\nabla T \cdot \nabla\psi}{|\nabla\psi|}\nabla\psi\right)\,, \tag{13}$$

with all terms being evaluated at the cell faces due to the staggered grid layout. The level set solver LIT and the flow solver NGA are coupled using the code coupling paradigm CHIMPS [14].

Results

In the following sections, verification and validation results for the surface force term, Eq. (13), implemented in the context of the finite-volume, balanced force approach are presented. In the first verification test, the thermocapillary motion of a drop in the limit of zero Marangoni number is compared to the creeping flow analytical solution of [3]. In the second test, the thermocapillary motion of a drop between a hot and a cold plate is analyzed and compared to experimental data.

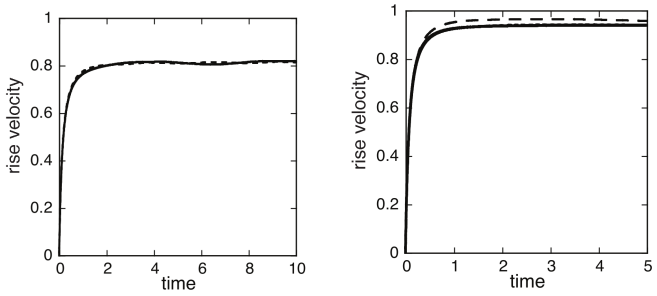

Figure 1. Normalized rise velocity of a (left) planar 2-D drop and (right) 3-D drop in the limit of vanishing Reynolds and Marangoni numbers: Grid sizes are $n_x = 64$ (dashed line), $n_x = 128$ (dotted line), $n_x = 256$ (solid line).

Thermocapillary migration of a drop in the limit of zero Marangoni number

The first test consists of a planar 2-D circular drop of diameter D of one fluid initially at rest in another fluid, both fluids having the same thermal diffusivity. The flow field is subjected to a time-invariant linear temperature profile, i.e., thermal conductivity is infinite and hence the Marangoni number is $Ma = 0$. The purpose of this test is to study the stability and accuracy of the proposed finite-volume, balanced force implementation of the Marangoni stress. In the limit of zero Marangoni number and small Reynolds number, [3] calculated the steady state velocity of a neutrally buoyant drop (sphere) in a constant temperature gradient field for two fluids of equal thermal conductivity to be $v_{\mathrm{YGB}} = -(\sigma_T G_T D)/(6\mu_b + 9\mu_d)$.

A drop of diameter $D = 1$ is placed inside a 2-D box of size $5D \times 7.5D$ [15], with the drop's center at the box centerline and $1.5D$ above the bottom wall. No-slip boundary conditions are imposed on the top and bottom wall, and periodic boundary conditions are used in the horizontal direction. A linear temperature field is imposed in the vertical direction, with $T = 0$ on the bottom wall and $T = 1$ on the top wall, resulting in $G_T = 0.1\overline{3}$. The fluid properties are $\rho_d = \rho_b = 0.2$, $\mu_b = \mu_d = 0.1$, $T_0 = 0$, $\sigma_0 = 0.1$, and $\sigma_T = -0.1$ [15]. Using these values, the theoretical rise velocity of a spherical drop is $v_{\mathrm{YGB}} = 8.88\overline{8} \times 10^{-3}$. In the simulations, the rise velocity v_r is calculated from

$$v_r = \frac{\int_V \psi v dV}{\int_V \psi dV} = \frac{\sum_{cv} \psi_{cv} v}{\sum_{cv} \psi_{cv}}, \tag{14}$$

where v is the vertical component of the velocity vector evaluated at the control volume centroid.

Figure 1 shows the temporal evolution of the numerically calculated rise velocity, normalized by v_{YGB}; equal resolution flow solver and G-grids were used. The 2-D solution converges to a value of $v_r/v_{\mathrm{YGB}} \approx 0.8$ (about 20% lower than the theoretical prediction for a spherical drop). Figure 1 (right) shows the normalized rise velocity for a sphere, calculated using the fully 3-D RLSG method. Again, grid convergence is observed, with the asymptotic value being $v_r/v_{\mathrm{YGB}} \approx 0.94$, comparable to the value of 0.97 obtained by [15] for the axisymmetric case. The difference in rise velocity between a planar 2-D drop and a spherical drop is significant.

In summary, the proposed method to include the Marangoni force into a balanced force finite-volume fluid solver using the RLSG front tracking approach yields stable results, comparable in accuracy to previously reported numerical results for axisymmetric flows.

Thermocapillary migration of a drop with finite Marangoni number

The second test consists of calculating the thermocapillary motion of a planar 2-D drop and a 3-D drop, at finite Marangoni numbers. Due to the finite Marangoni numbers, there is now a two-way coupling between the temperature equation and the Navier-Stokes equations. This is expected to result in a reduction of the tangential temperature gradients at the drop interface due to the interfacial flow driven by the Marangoni stress, which in turn will also be reduced.

Here, we aim to reproduce the experimental conditions reported in [6] and [7]. The domain consists of a $60\,\mathrm{mm} \times 45\,\mathrm{mm}(\times 45\,\mathrm{mm})$ rectangular box of no-slip walls. The bottom cold wall is held at a constant $T_0 = 283\,\mathrm{K}$, the top hot wall is held at a constant $T_1 = 343\,\mathrm{K}$, and the side walls are held at a time invariant linear temperature profile from T_0 at the bottom to T_1 at the top. At time $t = 0$, a circular (spherical) drop of diameter $D = 10.7\,\mathrm{mm}$ is released inside the bulk liquid. The drop's initial center is 15 mm from the

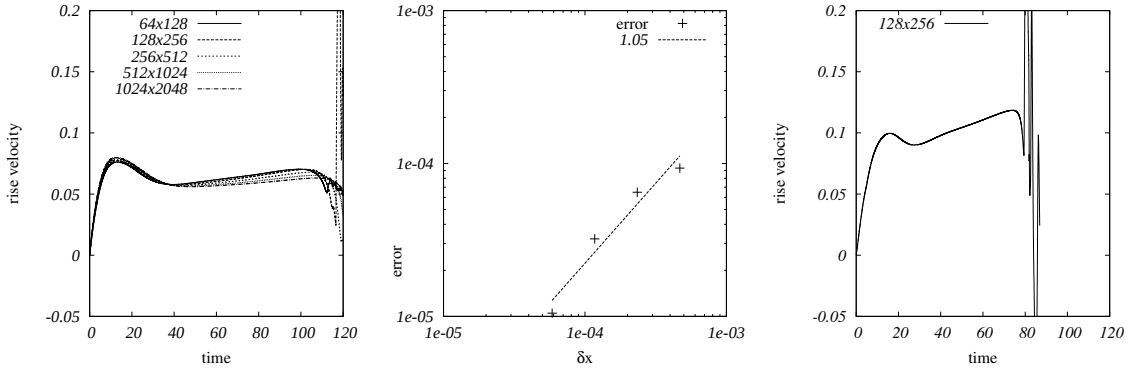

Figure 2. 2-D (left) and 3-D (right) non-dimensional rise velocity as function of employed grid resolution and resulting grid convergence in the 2-D case (center).

bottom. For the 2-D case, we use an idealized initial condition where the drop has the same initial linear temperature distribution as the bulk liquid. For the 3-D case, we hold the drop in place for 4.9 time units and use the more realistic condition of an isothermal drop.

For the surface tension between the two fluids, we use $\sigma_0 = 0.007$ N/m and $\sigma_T = -3.6 \times 10^{-5}$ N/m K. The density and viscosity variation with temperature of the two liquids are assumed to be of the form

$$\rho = A + BT\,, \qquad \mu = \exp(C + D/T), \tag{15}$$

where for the bulk $A = 1,200$ kg/m^3, $B = -0.9$ kg/K m^3, $C = -10.17$ and $D = 1,643$, and for the drop $A = 2,504$ kg/m^3, $B = -2.48$ kg/K m^3, $C = -11.76$ and $D = 1,540$. The thermal conductivity and the heat capacity of the bulk are set to a constant $k = 2.6778\,\mathrm{W/mK}$ and $c_p = 1778.2\,\mathrm{J/kgK}$, and that of the drop are $k = 1.26\,\mathrm{W/mK}$ and $c_p = 1047.0\,\mathrm{J/kgK}$. Using the above values and relations with a reference temperature of $T = 313\,\mathrm{K}$ (evaluated at the test cell center), the reference values of the analyzed case are $Re = 17.79$, $Ma = 86.15$, and $Pr = 4.84$.

At this point, a comment is in order with respect to the characteristic numbers found in atomizing liquid fuel jets with combustion. Assuming temperature differences of order 1500 K on length scales of 1 mm due to flames and liquid drop sizes of $R = 50\,\mu$m, the Reynolds number is $Re = 120$, the Prandtl number is $Pr = 0.66$, and the Marangoni number is $Ma = 80$. Although the Reynolds number is slightly larger than in the case analyzed here, the Marangoni number is virtually the same.

Figure 2 shows the scaled rise velocity of the drop as a function of non-dimensional time. The initial overshoot in the rise velocity is due to the imposed initial temperature gradient at the drop interface (2-D case). This initial transient behavior has been observed in other numerical simulations [e.g., 16]. Unfortunately, available experimental data is limited to the post-initial transient regime, so the observed behavior is difficult to validate. When the drop approaches the top wall, it slows down before impacting the wall, resulting in large deformation and ill defined rise velocities. Figure 2 (middle) also includes a grid convergence study for the 2-D case with respect to the peak rise velocity, using the finest grid rise velocity to estimate errors. First order convergence is observed.

Figure 3 shows snapshots of the isotherms at 4 different non-dimensionalized times for the 2-D and 3-D case using grid resolutions of 256×512 and $128\times128\times256$ respectively. The relatively benign isotherms inside the drop help maintain a significant temperature gradient at the phase interface, resulting in the relatively high rise velocity. As in the $Ma \to 0$ test problem analyzed in the previous section, the rise velocity of the planar 2-D drop is about 15% slower than that of a spherical drop.

Conclusions

Predicting flows dominated by surface tension is a challenging numerical task since discretization errors of this singular term can lead to large spurious currents. In this report, we have presented a numerical method to incorporate surface tension forces both normal and tangential to the phase interface in a consistent manner. The resulting method has been applied to the prediction of the thermocapillary motion of drops. Good agreement with theoretical predictions valid in the limit of zero Marangoni number are obtained.

For finite Marangoni and Reynolds numbers, complex transient behavior of the drop motion is observed. The Marangoni numbers studied in this case are close to those that may be expected for atomizing drops in

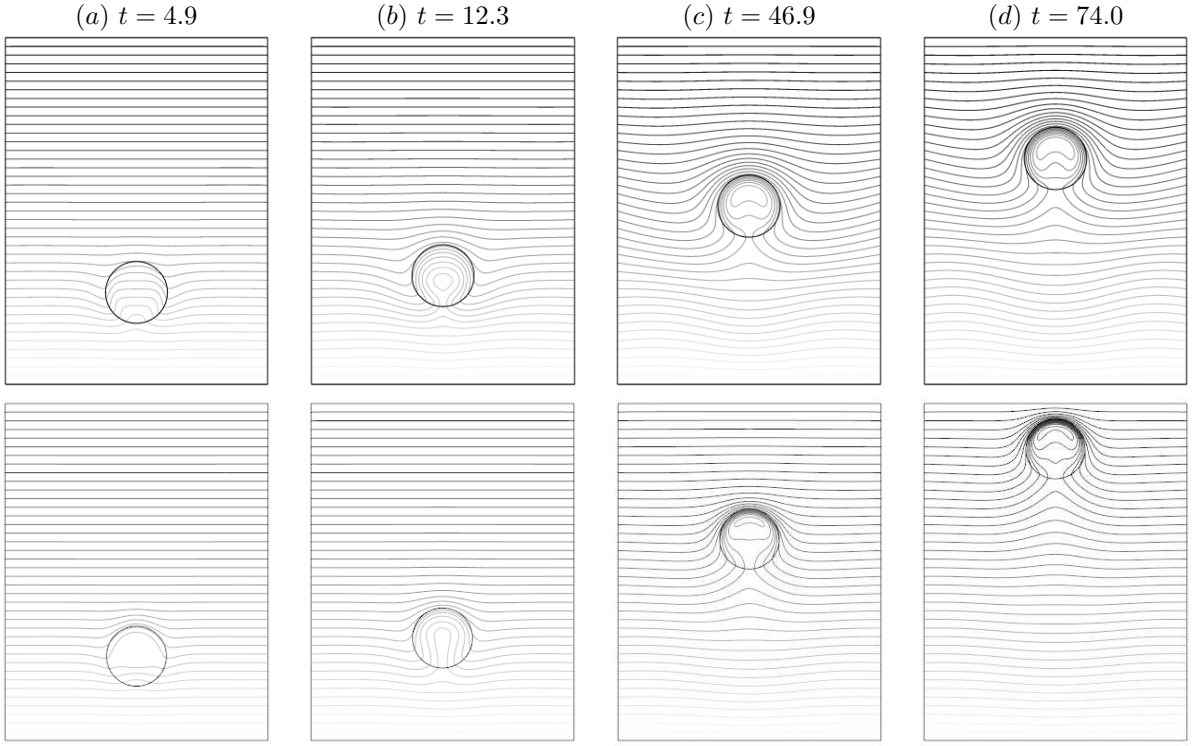

Figure 3. Isotherms for the planar 2-D case (top) and 3-D case in a plane through the center (bottom). $Re = 17.79$, $Ma = 86.15$, and $Pr = 4.84$.

combusting flows. Detailed numerical studies of the involved relative time scales and local aerodynamic forces to be performed in the future will answer the question whether thermocapillary effects during atomization are important. To this end, we have shown here that the proposed method provides a suitable approach.

Acknowledgments

This work was supported by NSF grant number DMS-0808045. The authors would like to thank M. Raessi for many helpful discussions.

References

[1] Levich, V.G. and Krylov, V.S. *Ann. Rev. Fluid Mech.* 1:293–316, 1969.
[2] Herrmann, M. *J. Comput. Phys.* 227(4):2674–2706, 2008.
[3] Young, N.O., Goldstein, J.S., et al. *J. Fluid Mech.* 6:350–356, 1959.
[4] Subramanian, R.S., Balasubramaniam, R., et al. In R. Monti, ed., *Physics of Fluids in Microgravity*, pages 149–177. London: Taylor and Francis, 2002.
[5] Treuner, M., Galindo, V., et al. *J. Colloid Interface Sci.* 179:114–127, 1996.
[6] Hadland, P.H., Balasubramaniam, R., et al. *Expt. Fluids* 26:240–248, 1999.
[7] Wozniak, G., Balasubramaniam, R., et al. *Expt. Fluids* 31:84–89, 2001.
[8] Landau, L.D. and Lifshitz, E.M. *Fluid Mechanics*. New York: Pergamon, 1959.
[9] Jiang, G.S. and Peng, D. *SIAM J. Sci. Comput.* 21(6):2126–2143, 2000.
[10] Shu, C.W. *SIAM J. Sci. Stat. Comput.* 9(6):1073–1084, 1988.
[11] Desjardins, O., Blanquart, G., et al. *J. Comput. Phys.* 227(15):7125–7159, 2008.
[12] Brackbill, J.U., Kothe, D.B., et al. *J. Comput. Phys.* 100:335–354, 1992.
[13] van der Pijl, S.P., Segal, A., et al. *Int. J. Numer. Meth. Fluids* 47:339–361, 2005.
[14] Alonso, J.J., Hahn, S., et al. In *42nd AIAA/ASME/SAE/ASEE Joint Propulsion Conference & Exhibit*, number 2006-5274 in AIAA-Paper. 2006.
[15] Muradoglu, M. and Tryggvason, G. *J. Comput. Phys.* 227:2238–2262, 2008.
[16] Yin, Z., Gao, P., et al. *Phys. Fluids* 20:082101, 2008.